JOURNAL OF SOLID STATE CHEMISTRY 77, 240–249 (1988)

On New Hydrated Fluorides of Trivalent Manganese

P. NUÑEZ,* A. TRESSAUD, J. DARRIET, AND P. HAGENMULLER

Laboratoire de Chimie du Solide du CNRS, Université de Bordeaux I, 351, cours de la Libération, 33405 Talence Cedex, France

AND W. MASSA, S. KUMMER, AND D. BABEL

Fachbereich Chemie der Philipps-Universität, D-3550 Marburg, Federal Republic of Germany

Received December 7, 1987; in revised form June 1, 1988

Three new hydrated fluorides of Mn^{3+} have been obtained from Ni^{2+} (or Cu^{2+}) and Mn^{3+} solutions in 40% hydrofluoric acid: $NiMnF_5 \cdot 7H_2O$, $CuMnF_5 \cdot 7H_2O$, and $Cu_3Mn_2F_{12} \cdot 12H_2O$. The monoclinic symmetries and the lattice constants of the two heptahydrates have been established. The crystal structure of $Cu_3Mn_2F_{12} \cdot 12H_2O$ has been refined using single-crystal X-ray diffraction data: it is triclinic with space group $P\bar{1}$ and parameters $a = 7.568(1)$ Å, $b = 7.558(1)$ Å, $c = 8.168(1)$ Å, $\alpha = 91.32°$, $\beta = 89.72°$, $\gamma = 92.61°$, $Z = 1$; $R = 0.046$ for 4040 independent reflections. It is isostructural with the homologous V, Cr, and Fe compounds. It can be considered as an inverse perovskite with formulation $[MnF_6][MnF_{6/2}][Cu(H_2O)_4F_{2/2}]_3$. Whereas the two heptahydrates are paramagnetic down to 2 K, a spontaneous magnetization occurs below $T_c = 3.8 \pm 0.2$ K for $Cu_3Mn_2F_{12} \cdot 12H_2O$. Hypotheses have been proposed to account for the field dependence of the magnetization by taking into account the superexchange mechanisms between two Jahn–Teller ions.

Compounds containing Mn^{3+} ions in octahedral coordination are generally associated with a cooperative Jahn–Teller effect. Ferro- or antiferrodistortive orderings result from particular arrangements of the outer *d* orbitals, yielding antiferro- or ferromagnetic couplings, respectively (*1*).

Further attractive features may arise from cationic orderings between trivalent manganese and other *d*-cations presenting a Jahn–Teller effect or not.

This research is devoted to the synthesis and the determination of the crystal structure and the magnetic properties of hydrated fluorides obtained from hydrofluoric acid solutions, in which Mn^{3+} is associated with either Ni^{2+} or Cu^{2+}. In the first system, only one compound has been obtained, $NiMnF_5 \cdot 7H_2O$, whereas, in the second, two phases have been characterized, $CuMnF_5 \cdot 7H_2O$ and $Cu_3Mn_2F_{12} \cdot 12H_2O$.

I. Experimental

A. Synthesis

$NiMnF_5 \cdot 7H_2O$. Mn_2O_3, prepared as described elsewhere (*2*), was dissolved in 40% HF solution. A solution of Ni^{2+} was obtained by dissolving $NiCO_3$ in the same re-

* Permanent address: Departamento de Quimica Inorganica, Universidad de La Laguna, Tenerife, España.

0022-4596/88 $3.00

agent. Both fresh warm solutions were mixed with an $Ni^{2+}:Mn^{3+}$ molar ratio of 1:1 and the resulting solution was allowed to stand overnight at room temperature. Red-brown crystals were grown which were successively washed in 40% hydrofluoric acid, in ethanol, and then dried in a water vapor free atmosphere. An identical process was tested for various $Ni^{2+}:Mn^{3+}$ molar ratios, i.e., from 4:1 to 1:4 at room temperature and at 50°C. In every case, the same crystalline phase was obtained, exhibiting identical X-ray powder patterns.

$CuMnF_5 \cdot 7H_2O$. A solution of CuF_2 (0.01 mole) in 40% hydrofluoric acid was mixed with a solution of Mn^{3+} (0.01 mole) prepared using the previously described method. Crystals were grown by very slow evaporation at room temperature for 2–3 weeks. The red-brown platelets were washed and dried as above. A similar phase was obtained with $Cu^{2+}:Mn^{3+}$ molar ratios varying from 2:1 to 1:2. The crystals exhibited dichroic properties and their color changed from red-brown to light-green by 90° rotation under polarizing light.

$Cu_3Mn_2F_{12} \cdot 12H_2O$. This phase was prepared under similar experimental conditions, but in this case the crystallization was carried out at slightly higher temperature (50°C). Crystals have a dark red color and have a block-like shape. They were obtained within the $Cu^{2+}:Mn^{3+}$ molar ratios 2:1 and 1:2.

B. Elemental Analysis

The content of the transition elements was determined by spectrophotometric methods and fluoride ions were titrated using an ion-selective electrode. The experiments were carried out at the Service Central d'Analyse du CNRS. The water content was obtained using a thermogravimetric technique. Typical dehydration curves are given in Fig. 1. Ten-milligram samples were set in a platinum crucible. The experiments were carried out in a flow of dry nitrogen at a heating rate of 50°C/hr. A change in the slope was observed in all cases slightly above 90°C; the heating process was stopped at about 100°C and the samples were let at this temperature for several hours to achieve the dehydration. For $CuMnF_5 \cdot 7H_2O$ (Fig. 1, curve b), the dehydration process started at lower temperature. A first change in the slope was noticed at about 70°C, which could correspond to the transitory occurrence of an intermediate hydrate. Analytical data of the three hydrates are given in Table I.

C. X-Ray Diffraction and Magnetic Characterizations

The crystal symmetries of the heptahydrates were obtained from Laue and Weissenberg photographs. Their lattice constants were refined at room temperature from powder patterns with internal stan-

TABLE I

ANALYTICAL DATA

Compound		Ni	Cu	Mn	F	H_2O
$NiMnF_5 \cdot 7H_2O$	exp. (%)	17.5	—	16.1	27.6	37.3
	calc. (%)	17.5		16.4	28.4	37.7
$CuMnF_5 \cdot 7H_2O$	exp. (%)	—	18.2	15.6	27.5	35.4
	calc. (%)		18.7	16.2	27.9	37.1
$Cu_3Mn_2F_{12} \cdot 12H_2O$	exp. (%)	—	24.8	14.2	30.2	29.0
	calc. (%)		25.6	14.7	30.6	29.0

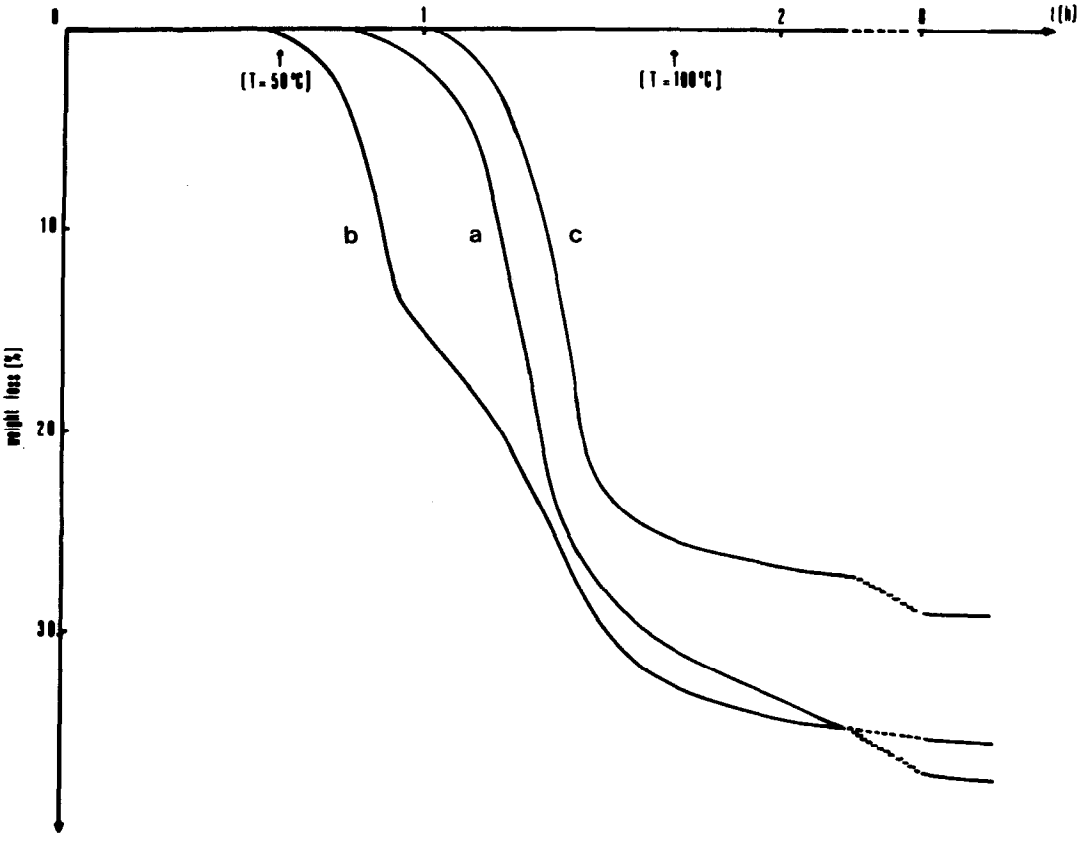

FIG. 1. Dehydration curves of $NiMnF_5 \cdot 7H_2O$ (a), $CuMnF_5 \cdot 7H_2O$ (b), and $Cu_3Mn_2F_{12} \cdot 12H_2O$ (c).

dards. The crystal structure of $Cu_3Mn_2F_{12} \cdot 12H_2O$ was determined on a 4-circle diffractometer (CAD4, Enraf–Nonius, Mo$K\alpha$; graphite monochromator). The unit-cell constants were refined from 25 high-angle reflections. The crystallographic data of the three phases are grouped in Table II.

The magnetic characterization was car-

TABLE II

CRYSTALLOGRAPHIC DATA

	$NiMnF_5 \cdot 7H_2O$	$CuMnF_5 \cdot 7H_2O$	$Cu_3Mn_2F_{12} \cdot 12H_2O$
Symmetry:	Monoclinic $C2/m$	Monoclinic $P2_1/c$	Triclinic $P\bar{1}$
Lattice constants (room temperature)	a = 11.089(5) Å b = 14.063(5) Å c = 6.375(5) Å β = 100.39°	a = 8.979(5) Å b = 18.237(5) Å c = 6.010(5) Å β = 96.40°	a = 7.569(1) Å α = 91.32° b = 7.558(1) Å β = 89.72° c = 8.168(1) Å γ = 92.61°
$\rho_{exp.}$ (g · cm^{-3})	2.26 ± 0.02	2.34 ± 0.02	2.65 ± 0.02
$\rho_{calc.}$ (g · cm^{-3})	2.27 (Z = 4)	2.31 (Z = 4)	2.66 (Z = 1)

ried out from 1.8 to 300 K using a Faraday-type microbalance and a Squid magnetometer. Magnetic fields were applied up to 6 T.

II. Lattice Constants of the Heptahydrates $NiMnF_5 \cdot 7H_2O$ and $CuMnF_5 \cdot 7H_2O$

Hydrated fluorides with $M^{II}M'^{III}F_5 \cdot 7H_2O$ formulation have been found for most 3*d*-elements having stable divalent and/or trivalent oxidation states. Their dehydration processes have been widely investigated since the early works of Petersen (*3–7*). Although these phases have been characterized using numerous physical methods—in particular magnetic and Mössbauer studies on Fe-based compounds (*8–10*)—the determination of the unit cell and symmetry is still a subject of controversy.

Gallagher and Ottaway (*11*) have proposed for several members of the series a triclinic symmetry with lattice constants of about $a \simeq 6.5$ Å, $b \simeq 8.9$ Å, $c \simeq 10.4$ Å, $\alpha \simeq 106°$, $\beta \simeq 123°$, $\gamma \simeq 83°$. These proposals are essentially based on precession photograph data of $Fe_2F_5 \cdot 7H_2O$ (*5*). On the other hand Bukhvetskii *et al.* (*14*) determined the complex structure of $ZnInF_5 \cdot 7H_2O$ in which $[Zn(H_2O)_6]$, $[InF_6]$, and $[InF_4(H_2O)_2]$ units are present.

The only complete structural analysis carried out on a single crystal of a transition-metal-based heptahydrate has been performed by Massa on $CoAlF_5 \cdot 7H_2O$ (*12, 13*). The structural network is formed of arrangements of $[Co(H_2O)_6]$ and $[AlF_5(H_2O)]$ octahedra in which F anions and H_2O groups are disordered. These octahedra are connected by a three-dimensional array of hydrogen bonds.

A comparison of the symmetry (*C*2/*m*) and lattice constants of $CoAlF_5 \cdot 7H_2O$, $a = 10.917$ Å, $b = 13.863$ Å, $c = 6.525$ Å, $\beta = 100.3°$, with those of $NiMnF_5 \cdot 7H_2O$ clearly shows these two phases to be isostructural. The indexation of the X-ray powder pattern of $NiMnF_5 \cdot 7H_2O$ is given in Table III together with that of $CuMnF_5 \cdot 7H_2O$. One may notice that the new type of unit cell characterizing the latter compound might be due to the presence of two Jahn–Teller ions in the structure.

III. Crystal Structure of $Cu_3Mn_2F_{12} \cdot 12H_2O$

Data collection was carried out on a dark-red crystal of $Cu_3Mn_2F_{12} \cdot 12H_2O$ of dimensions $0.20 \times 0.13 \times 0.05$ mm^3 by ω-scans corresponding to $0.9 + 0.35 \tan \theta$ and to additional 25% on each side of the reflection for background determination. In the range $1° < \theta < 40°$ of the $+h$, $\pm k$, $\pm l$ octants, 5975 reflections have been measured to yield 5640 independent reflections ($R_{int.} = 2.3\%$); 4040 of them with $F_o > 5\sigma$ were used for full-matrix refinement (*15–17*). A numerical absorption correction has been applied (absorption coefficient $\mu = 47$ cm^{-1}). The atomic parameters of the isotypic iron phase (*18*) were chosen as starting set. Scattering factors were taken from (*19*) and the influence of anomalous dispersion (*20*) was included. Anisotropic temperature factors were refined for all atoms except hydrogen. The water molecules were treated as rigid groups (O–H, 0.75 Å; H–O–H, 104.4°) and isotropic thermal parameters were refined for the H atoms. An extinction correction $F_c(\text{corr}) = F_c(1 - \varepsilon F_c^2/\sin \theta)$ was applied with ε refined to 1.6×10^{-6}. Based on the minimalized function $\Sigma w(|F_o| - |F_c|)^2$, where w is $1/\sigma^2(F_o)$, the weighted R factor converged to $R_w = 0.0461$ and the conventional R factor to $R = 0.0459$.

The resulting positional and equivalent isotropic temperature factors are given in Table IV, selected interatomic distances and angles in Table V.

The structure of $Cu_3Mn_2F_{12} \cdot 12H_2O$ is similar to those of the homologous phases with M(III) = V, Cr, or Fe (*18*). The pres-

TABLE III

X-RAY POWDER PATTERNS OF $NiMnF_5 \cdot 7H_2O$ (A) AND $CuMnF_5 \cdot 7H_2O$ (B)

$I_{obs.}$	$d_{obs.}$ (Å)	$d_{calc.}$ (Å)	$h\,k\,l$	$I_{obs.}$	$d_{obs.}$ (Å)	$d_{calc.}$ (Å)	$h\,k\,l$
		A					
S	4.73	4.758	1 1 1	W	2.225	2.228	4 2 1
S	4.67	4.680	0 2 $\bar{1}$			2.225	3 5 0
VS	4.53	4.540	2 0 $\bar{1}$	VW	2.206	2.196	0 6 $\bar{1}$
VS	4.30	4.309	2 2 0	M	2.163	2.160	4 2 $\bar{2}$
		4.307	1 3 0			2.160	5 1 $\bar{1}$
S	3.79	3.790	2 0 1			2.159	3 1 2
M	3.53	3.520	3 1 0	W	2.022	2.027	3 5 1
M	3.15	3.135	0 0 $\bar{2}$	W	2.013	2.012	1 5 2
VW	3.10	3.091	1 1 $\bar{2}$	VW	1.973	1.973	5 3 0
M	2.865	2.863	0 2 2			1.976	1 7 $\bar{0}$
		2.863	3 1 $\bar{1}$	W	1.911	1.907	4 4 $\bar{2}$
S	2.780	2.780	2 4 $\bar{1}$	W	1.904	1.902	1 7 $\bar{1}$
VW	2.741	2.727	2 2 $\bar{2}$	W	1.896	1.895	4 0 2
		2.727	4 0 $\bar{0}$	W	1.850	1.843	2 0 $\bar{3}$
W	2.577	2.576	3 1 $\bar{2}$	W	1.825	1.825	4 0 $\bar{3}$
		2.576	2 4 $\bar{1}$	VW	1.810	1.812	5 3 $\bar{2}$
VW	2.534	2.540	1 5 $\bar{1}$	W	1.794	1.797	0 4 $\bar{3}$
S	2.496	2.509	4 2 $\bar{1}$	M	1.767	1.767	4 2 $\bar{3}$
M	2.385	2.379	2 2 $\bar{2}$			1.766	4 6 $\bar{1}$
W	2.265	2.272	4 0 $\bar{2}$				
		2.264	2 4 $\bar{2}$				
		B					
VW	5.04	5.037	1 1 $\bar{1}$	W	2.283	2.287	2 2 $\bar{2}$
		5.024	1 3 0			2.285	1 5 $\bar{2}$
VS	4.56	4.575	1 1 1			2.281	1 7 1
		4.559	0 4 $\bar{0}$			2.280	0 8 0
		4.544	1 2 $\bar{1}$	VW	2.202	2.202	2 3 $\bar{2}$
S	4.46	4.462	2 0 0	VW	2.154	2.155	4 1 $\bar{1}$
S	4.19	4.196	1 2 $\bar{1}$			2.130	0 6 2
VW	3.97	3.969	1 3 $\bar{1}$	VW	2.129	2.130	0 8 $\bar{1}$
S	3.19	3.189	2 4 0			2.128	2 5 $\bar{2}$
		3.184	2 2 1	W	2.111	2.112	4 2 $\bar{1}$
W	2.986	2.986	0 0 2			2.110	1 6 $\bar{2}$
W	2.944	2.947	0 1 2	VW	2.090	2.091	3 5 $\bar{1}$
W	2.881	2.887	1 5 1			2.090	1 8 $\bar{1}$
		2.877	1 6 0	W	2.055	2.055	3 6 $\bar{1}$
W	2.824	2.828	3 2 0			2.053	1 8 1
		2.824	2 5 $\bar{0}$	W	2.031	2.030	2 8 $\bar{0}$
M	2.790	2.791	1 2 $\bar{2}$			2.007	3 4 $\bar{2}$
VW	2.740	2.741	1 0 2	VW	2.003	2.005	4 1 1
W	2.711	2.711	1 1 $\bar{2}$			2.004	4 4 0
		2.709	0 6 1			1.999	3 0 $\bar{2}$
W	2.680	2.680	0 3 $\bar{2}$			1.985	2 6 $\bar{2}$
W	2.640	2.641	1 3 $\bar{2}$	W	1.983	1.983	2 5 2
M	2.620	2.620	2 0 $\bar{2}$			1.979	0 1 $\bar{3}$
W	2.598	2.594	2 1 $\bar{2}$			1.979	1 1 $\bar{3}$
W	2.555	2.556	1 6 $\bar{1}$			1.954	3 6 1
VW	2.535	2.535	3 3 $\bar{1}$	M	1.954	1.953	3 2 $\bar{2}$
		2.501	1 7 0			1.952	2 8 $\bar{1}$
W	2.499	2.499	1 3 2				
		2.498	0 4 2				

Note. VS: very strong; S: strong; M: medium; W: weak; VW: very weak.

ence of a second Jahn–Teller ion (d^4 high-spin Mn^{3+}) leads only to minor modifications. $[MnF_6]$ groups are connected via planar $[Cu(H_2O)_4]$ units in three directions (Fig. 2) to form a pseudocubic network of corner-connected $[MnF_{6/2}]$ and *trans*-$[Cu(H_2O)_4F_{2/2}]$ octahedra. In the center of each pseudocube an additional isolated $[MnF_6]$ group is located. To emphasize the anti-perovskite-type relation (*18*) the formula may be written: $[MnF_6][MnF_{6/2}][Cu(H_2O)_4F_{2/2}]_3$. Both $[MnF_6]$ octahedra show the typical elongation which characterizes the Jahn–Teller effect, as do the $[Cu(H_2O)_4F_{2/2}]$ octahedra along their F–Cu–F axis.

The elongated axes of the $[MnF_6]$ octahedra at the corners of the pseudocube show ferrodistortive ordering along the

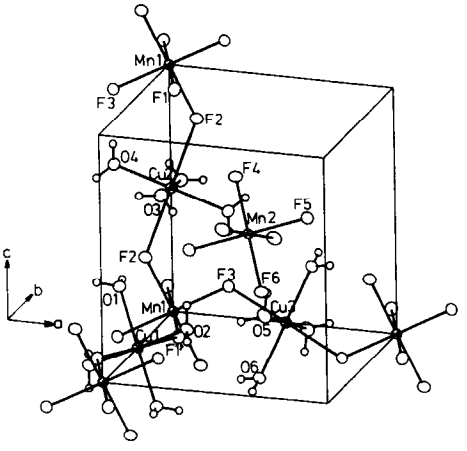

FIG. 2. Structural arrangement of $[CuF_{2/2}(H_2O)_4]$ and $[MnF_6]$ octahedra in $Cu_3Mn_2F_{12} \cdot 12H_2O$ (origin shifted by 0, 1/2, 0).

TABLE IV

FRACTIONAL COORDINATES AND TEMPERATURE FACTORS FOR $Cu_3Mn_2F_{12} \cdot 12H_2O$

Atom	x	y	z	U_{11}	U_{22}	U_{33}	U_{23}	U_{13}	U_{12}
Cu1	.0000	.0000	.0000	.0204(2)	.0159(2)	.0167(2)	−.0005(1)	−.0022(1)	.0007(1)
Cu2	.0000	.5000	.5000	.0214(2)	.0173(2)	.0187(2)	.0006(1)	−.0007(1)	.0004(1)
Cu3	.5000	.5000	.0000	.0223(2)	.0176(2)	.0181(2)	.0005(1)	−.0022(1)	.0016(1)
Mn1	.0000	.5000	.0000	.0179(2)	.0127(2)	.0167(2)	.0006(1)	−.0013(2)	.0002(1)
Mn2	.5000	.0000	.5000	.0189(2)	.0149(2)	.0149(2)	.0004(2)	−.0011(2)	.0003(2)
F1	.0924(2)	.2831(2)	.9706(2)	.0277(8)	.0151(6)	.0325(8)	.0008(6)	.0022(6)	.0023(5)
F2	.0958(2)	.5743(2)	.7690(2)	.0310(8)	.0222(7)	.0214(7)	−.0003(5)	−.0016(6)	.0024(6)
F3	.2220(2)	.5867(2)	.0939(2)	.0233(7)	.0279(7)	.0244(8)	−.0010(6)	−.0018(6)	−.0004(6)
F4	.4187(3)	.0891(2)	.7023(2)	.0345(9)	.0249(7)	.0229(8)	−.0050(6)	.0026(7)	.0018(6)
F5	.2392(2)	.9931(2)	.4140(2)	.0251(8)	.0342(9)	.0247(8)	−.0009(7)	−.0034(6)	.0019(6)
F6	.4584(3)	.7740(2)	.5783(2)	.043(1)	.0181(7)	.0263(8)	.0042(6)	−.0045(7)	−.0025(6)
O1	.1019(3)	.9248(3)	.7884(3)	.030(1)	.0214(8)	.0218(9)	−.0008(7)	.0028(7)	−.0011(7)
O2	.2310(3)	.9645(3)	.1041(3)	.028(1)	.0234(8)	.0227(9)	−.0028(7)	−.0061(7)	.0046(7)
O3	.0349(3)	.2492(3)	.5437(3)	.032(1)	.0198(8)	.031(1)	.0008(7)	.0038(8)	.0020(7)
O4	.2448(3)	.5238(3)	.4190(3)	.025(1)	.032(1)	.025(1)	.0001(8)	.0024(7)	−.0017(7)
O5	.4810(3)	.2594(3)	.0929(3)	.038(1)	.0250(9)	.027(1)	.0060(8)	−.0063(8)	−.0069(8)
O6	.4039(3)	.4230(3)	.7872(3)	.0254(9)	.0237(8)	.0229(9)	−.0026(7)	−.0025(7)	.0018(7)
H1	.1894(3)	.9696(3)	.7659(3)	.04(1)					
H2	.1198(3)	.8275(3)	.7872(3)	.04(1)					
H3	.2304(3)	.9693(3)	.1963(3)	.06(2)					
H4	.2612(3)	.8729(3)	.0834(3)	.10(3)					
H5	.1022(3)	.1982(3)	.4963(3)	.05(1)					
H6	−.0423(3)	.1838(3)	.5538(3)	.08(2)					
H7	.2401(3)	.5480(3)	.3302(3)	.06(2)					
H8	.3000(3)	.5983(3)	.4584(3)	.09(2)					
H9	.4937(3)	.2616(3)	.1844(3)	.04(1)					
H10	.3983(3)	.2016(3)	.0796(3)	.08(2)					
H11	.3135(3)	.4532(3)	.7658(3)	.05(1)					
H12	.4030(3)	.3277(3)	.7580(3)	.06(2)					

c-direction, but the lengthening of this axis with respect to a and b is already present to a similar extent in the compounds containing trivalent non-Jahn–Teller cations. The elongation must be ascribed, therefore, to the influence of hydrogen bonds (Table VI) which are strongest toward the F2 ions bridging Mn^{3+} and Cu^{2+} ions along the c-direction. The F3 ions which constitute bridges in the direction of the a-axis are considerably less involved in hydrogen bonding and the F1 ions (bridging in the b-direction) are not at all. The hydrogen bond topology appears to be essentially the same as in the V, Cr, and Fe compounds (*18*).

The isolated $[MnF_6]$ unit at the center exhibits essentially the same elongation as the corresponding groups within the framework, but with its long axis pointing in the a-direction. Thus the a parameter (a = 7.568 Å) which in the Cr, V, and Fe compounds is the shortest one (a = 7.468, 7.508, and 7.504 Å) becomes even slightly longer than the b parameter (b = 7.558 Å compared with 7.595, 7.607, and 7.612 Å for the Cr, V, and Fe phases, respectively).

IV. Magnetic Properties

1. $NiMnF_5 \cdot 7H_2O$ and $CuMnF_5 \cdot 7H_2O$

The two heptahydrates follow a Curie law in the temperature range 2.2–300 K as

TABLE V

SELECTED INTERATOMIC DISTANCES (Å) AND ANGLES (DEG) IN $Cu_3Mn_2F_{12} \cdot 12H_2O$.

Mn1–F1	1.822(2)	Cu1–O1	1.972(2)
Mn1–F2	2.098(2)	Cu1–O2	1.979(2)
Mn1–F3	1.931(2)	Cu1–F1	2.239(2)
Mn2–F4	1.882(2)	Cu2–O3	1.967(2)
Mn2–F5	2.096(2)	Cu2–O4	1.966(2)
Mn2–F6	1.851(2)	Cu2–F2	2.364(2)
Mean Mn–F_{ax}	2.097	Cu3–O5	1.986(2)
Mn–F_{eq}	1.872	Cu3–O6	1.953(2)
Mn–F	1.947	Cu3–F3	2.352(2)
Mean Cu–O	1.971	O1–Cu1–O2	88.9(1)
Cu–F	2.318	O1–Cu1–F1	86.8(1)
		O2–Cu1–F1	93.1(1)
F1–Mn1–F2	90.0(1)	O3–Cu2–O4	90.6(1)
F1–Mn1–F3	90.9(1)	O3–Cu2–F2	89.2(1)
F2–Mn1–F3	91.1(1)	O4–Cu2–F2	89.4(1)
F4–Mn2–F5	91.1(1)	O5–Cu3–O6	94.2(1)
F4–Mn2–F6	88.2(1)	O5–Cu3–F3	95.7(1)
F5–Mn2–F6	88.9(1)	O6–Cu3–F3	92.1(1)
Mn1–F1–Cu1	136.86(9)	Mn1–F2–Cu2	132.42(8)
Mn1–F3–Cu3	123.86(8)		

Note. All cations are situated at a center of symmetry.

shown in Fig. 3. The Curie constants have been deduced from the thermal variation of the molar susceptibilities corrected for diamagnetism. The values of the susceptibilities are consistent with those of two independent paramagnetic ions. The experimental C_m are compared below with calculated ones using theoretical spin-only values of the individual ions and an average $\bar{g}$ value of 2.24 for Cu^{2+}:

	θ_p (±2 K)	C_m (exp.)	C_m (calc.)
$NiMnF_5 \cdot 7H_2O$	0	4.32	4.0
$CuMnF_5 \cdot 7H_2O$	0	3.51	3.47

It may be noticed that below 4 K neither a minimum value has been observed in the $\chi^{-1} = f(T)$ curves—as noted for $Fe_2F_5 \cdot 7H_2O$ and $FeCoF_5 \cdot 7H_2O$ (*21*)—nor a field dependency of the magnetization. Mn^{3+} ions in octahedral coordination (with $t_{2g}^3 d_{z^2}^1$ $d_{x^2-y^2}^0$ electronic configuration) exhibit a Jahn–Teller effect generally associated with an ordering of the d_{z^2} orbitals. This ordering, which gives rise to the presence of only one unpaired electron along one of the bonding directions, weakens the Mn^{3+}–X. . .X–M^{2+} superexchange interactions relative to those observed along all axes for either $Fe^{3+}(t_{2g}^3 e_g^2)$ or $Co^{3+}(t_{2g}^4 e_g^2)$.

2. $Cu_3Mn_2F_{12} \cdot 12H_2O$

The thermal dependency of the reciprocal susceptibility is given in Fig. 4. In the concerned temperature range, a linear variation is observed with a very small θ_p value. The experimental Curie constant (C_m(exp.) = 7.40) is in excellent agreement with that calculated using spin-only values of the individual ions and the average $\bar{g}$ value of 2.24 for Cu^{2+} (C_m(calc.) = 7.41). Below 4 K a spontaneous magnetization M_0 occurs when the material is zero-field cooled. The ordering temperature $T_C = 3.8 \pm 0.2$ K can be obtained from the $M_0 = f(T)$ curve given in Fig. 4. The field dependency of the magnetization is shown in Fig. 5: the experimental values have been measured at dif-

TABLE VI

HYDROGEN BONDS [d(O. . .F) < 2.8 Å] IN $Cu_3Mn_2F_{12} \cdot 12H_2O$

		d(O. . .F) (Å)	O–H–F (deg)
At Cu1	O1–H1. . .F4	2.745	179
	O1–H2. . .F2	2.648	164
	O2–H3. . .F5	2.536	176
At Cu2	O3–H5. . .F5	2.724	160
	O3–H6. . .F5′	2.729	178
	O4–H7. . .F3	2.716	174
	O4–H8. . .F6	2.741	173
At Cu3	O5–H9. . .F6	2.746	170
	O6–H11. . .F2	2.650	163
	O6–H12. . .F4	2.609	174
Mean	O–H. . .F	2.684	171

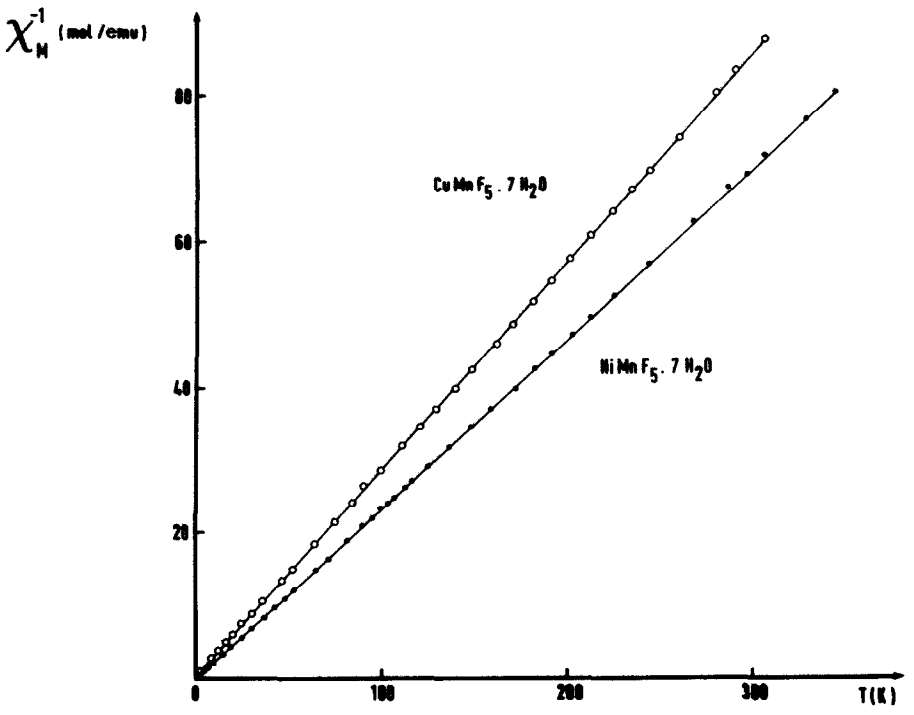

FIG. 3. Thermal dependency of the reciprocal molar susceptibility of $NiMnF_5 \cdot 7H_2O$ and $CuMnF_5 \cdot 7H_2O$.

ferent temperatures for magnetic fields decreasing from 50 kOe to zero.

As explained above, the structure can be described as a 3D-network of ordered $[Cu(H_2O)_4F_{2/2}]$ and $[MnF_{6/2}]$ octahedra sharing 2 and 6 vertices, respectively. The formula of this arrangement is $Cu_3MnF_6(H_2O)_{12}$ and it is completed by an additional isolated $[MnF_6]$ octahedron occupying the center of the pseudo-cube. Magnetic couplings in 3D fluorides can be largely explained using the Goodenough–Kanamori superexchange rules (*22*). However, one of the critical points is the dependence on *M*–F–*M* bridging angles, 180° being the optimum case. Pebler *et al.* (*23*) recently showed the influence of angle deviation on the value of the exchange constants in Mn^{3+} fluorides.

Although in the present case the angular deviation from 180° may attain 56°, ferromagnetic superexchange couplings can be expected to occur between filled d_{z^2} Cu^{2+} orbitals and half-filled d_{z^2} Mn^{3+} orbitals via the fluorine *p* orbitals along the *c*-axis. These interactions which could be enhanced by stronger hydrogen bonds might lead to ferromagnetic –Mn–Cu–Mn– chains coupled antiferromagnetically via empty $d_{x^2-y^2}$ orbitals of Mn^{3+} and filled d_{z^2} orbitals of Cu^{2+}. In such an assumption, the resulting moment, calculated in the colinear model would be of 1 μ_B $mole^{-1}$ from the spin-only moment conditions. Although a close value is observed at 1.95 K for the remanent magnetization ($M \simeq 0.9$ μ_B $mole^{-1}$ in Fig. 5), it results from the value of the extrapolated zero-field moment ($M \simeq 4$ μ_B $mole^{-1}$) and from the absence of a further saturation up to 50 kOe that a more

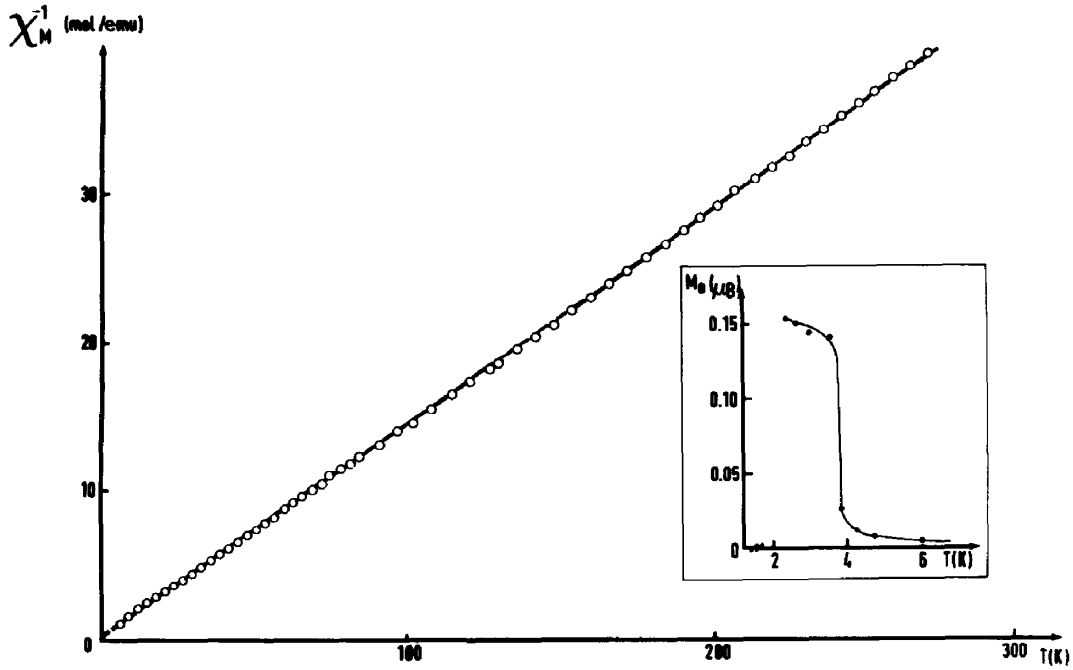

FIG. 4. Thermal dependency of the reciprocal molar susceptibility and spontaneous magnetization of $Cu_3Mn_2F_{12} \cdot 12H_2O$.

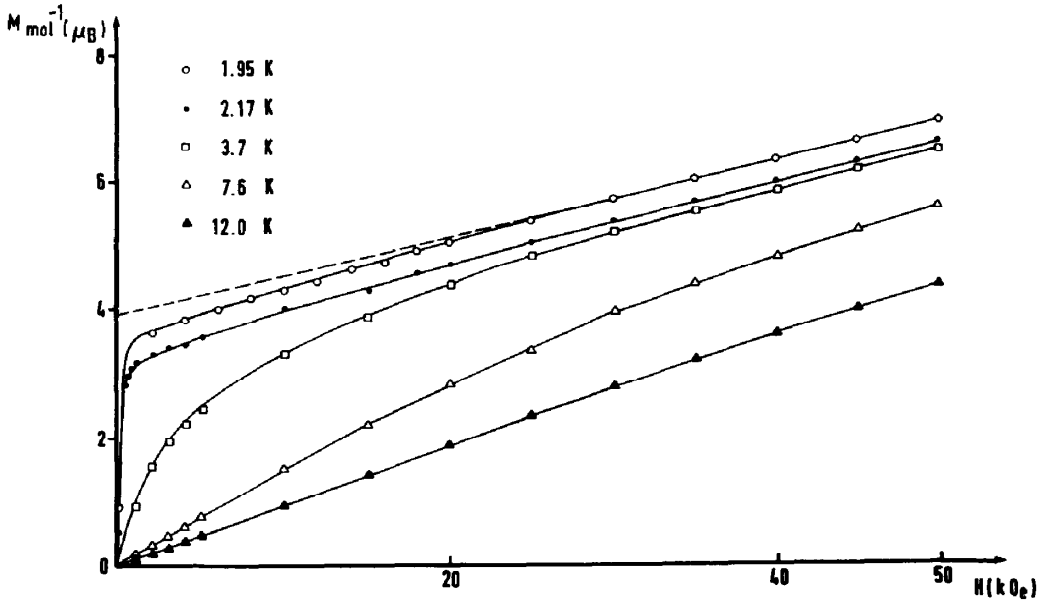

FIG. 5. Field dependency of the molar magnetization of $Cu_3Mn_2F_{12} \cdot 12H_2O$.

complex model can be sought. Noncolinear models involving either ferrimagnetic interactions or antiferromagnetic ones between next nearest neighbors could be taken into account. The synthesis of a deuterated material is in progress in order to determine the magnetic structure by neutron diffraction.

Acknowledgment

This work has been carried out as part of a European Stimulation Research Program.

References

1. D. Reinen and C. Friebel, *Struct. Bonding (Berlin)* **37,** 1 (1979).
2. T. E. Moore, M. Ellis, and P. E. Selwood, *J. Amer. Chem. Soc.* **72,** 856 (1950).
3. E. Petersen, *J. Prakt. Chem.* **40,** 58 (1889).
4. G. Brauer and M. Eichner, *Z. Anorg. Allg. Chem.* **296,** 1 (1958).
5. K. J. Gallagher and M. R. Ottaway, *J. Chem. Soc. Dalton Trans.* 978 (1975).
6. D. B. Brown and E. G. Walton, *J. Chem. Soc. Dalton Trans.* 845 (1980).
7. E. G. Ippolitov and T. A. Tripol'skaya, *Russ. J. Inorg. Chem.* **25,** 425 (1980).
8. T. Sakai and T. Tominaga, *Radiochem. Radioanal. Lett.* **22,** 11 (1975).
9. E. G. Walton, P. J. Corvan, D. B. Brown, and P. Day, *Inorg. Chem.* **15,** 1737 (1976).
10. P. Imbert, Y. Macheteau, and F. Varret, *J. Phys.* **34,** 49 (1973).
11. K. J. Gallagher and M. R. Ottaway, *J. Chem. Soc. Dalton,* 2212 (1977).
12. W. Massa, *J. Fluorine Chem.* **16,** 634 (1980).
13. W. Massa, Habilitationschrift, Univ. Marburg, FRG (1982).
14. B. V. Bukhvetskii, S. A. Polytshuk, and V. I. Simonov, *Koord. Khim.* **3,** 926 (1977).
15. R. E. Schmidt, M. Birkhahn, and W. Massa, "STRUX, Programmsystem zur Verarbeitung von Röntgendaten," Marburg (1980).
16. G. M. Sheldrick, "SHELX76, Program for Crystal Structure Determination," Cambridge (1976).
17. C. K. Johnson, "ORTEP, A Fortran Thermal-Ellipsoid Plot Program for Crystal Structure Illustrations," Report ORNL-3794, Oak Ridge, TN (1965).
18. S. Kummer and D. Babel, *Z. Naturforsch. B* **42,** 1403 (1987).
19. D. T. Cromer and J. D. Mann, *Acta Crystallogr. Ser. A* **24,** 321 (1968).
20. D. T. Cromer and D. Liberman, *J. Chem. Phys.* **53,** 1891 (1970).
21. E. R. Jones, M. E. Hendricks, T. Auel, and E. L. Amma, *J. Chem. Phys.* **66,** 3252 (1977).
22. A. Tressaud and J. M. Dance, *Adv. Inorg. Chem. Radiochem.* **20,** 133 (1977).
23. J. Pebler, W. Massa, H. Lass, and B. Ziegler, *J. Solid State Chem.* **71,** 87 (1987).